

# DESIGN OF A COMPACT SUPERCONDUCTING CRAB-CAVITY FOR LHC USING Nb-ON-Cu-COATING TECHNIQUE

A. Grudiev<sup>1,\*</sup>, S. Atieh<sup>1</sup>, R. Calaga<sup>1</sup>, S. Calatroni<sup>1</sup>, O. Capatina<sup>1</sup>, F. Carra<sup>1,2</sup>, G. Favre<sup>1</sup>,  
L.M.A. Ferreira<sup>1</sup>, J.-F. Poncet<sup>1</sup>, T. Richard<sup>1</sup>, A. Sublet<sup>1</sup>, C. Zanoni<sup>1</sup>,  
<sup>1</sup>CERN, Geneva, Switzerland; <sup>2</sup>Politecnico di Torino, Turin, Italy

## Abstract

The design of a compact superconducting crab-cavity for LHC using Nb-on-Cu-coating technique is presented. The cavity shape is based on the ridged waveguide resonator with wide open apertures to provide access to the inner surface of the cavity for coating. It also provides natural damping for HOMs and rather low longitudinal and transverse impedances. The results of the cavity shape optimization taking into account RF performance, coating, and thermo-mechanical considerations, as well as the design and fabrication plans of the first prototype for coating and cold tests are presented.

## INTRODUCTION

The upgrade of the LHC to a higher luminosity (HL-LHC) [1], among the other things, includes using so-called crab cavities which are RF deflecting cavities operating at zero crossing and tilting the LHC bunches before and after collision point in order to provide head-on collisions. For LHC, due to requirements for RF frequency to be 400 MHz and due to given distance between the two beam pipes at the foreseen cavity locations of about 194 mm, the crab cavity transverse dimension must be significantly smaller than half of the wavelength. This requires compact cavity shapes to be used that are rather different from standard elliptical pill-box cavity type. A number of compact SRF crab cavities have been designed for LHC based on the solid Nb manufacturing technology in the framework of HL-LHC program [2].

Nevertheless, there is an alternative SRF technology based on the Nb-on-Cu-coating technique developed to large extent at CERN for the largest ever-built SRF system of LEP2 at CERN. Although typically solid Nb SRF cavities show lower surface RF power loss and require less cryogenic power for cooling than Nb-on-Cu cavities, the latter ones do not have so-called quenching, a physical phenomenon related to thermal runaway process in the bulk Nb due to its relatively low thermal conductivity. On the contrary, Cu with its high thermal conductivity provides very good cooling of the superconducting Nb thin film on the cavity surface. In addition, Cu offers a possibility to create much more complex and much more accurate cavity shapes by using modern CNC 5-axis milling machines than solid Nb sheet technology. This advantage is rather important in the compact crab cavity design, whereas higher cryogenic loss can probably be accepted as it is already the case for the LHC main RF

\*Alexej.Grudiev@cern.ch

system. Last but not least, much thicker Cu cavity walls significantly reduce cavity frequency sensitivity both to the external liquid He bath pressure variations and to the Lorentz force detuning.

In this paper, we describe the design of a prototype which addresses the feasibility issues of fabrication and coating of the cavity itself with the final goal of measuring the RF power loss at 4.5 K as a function of the cavity voltage in a general purpose cryostat. No fundamental mode coupler nor HOM couplers are addressed in the prototype and are left for the future work as well as the design of a dedicated cryostat for possible beam tests.

## RF DESIGN

The shape of the internal surface of the cavity is directly related both to its RF performance and to the Nb-coating process. One can be adapted to the needs of the other one and vice-a-versa. The existing designs of the LHC crab cavity make it very difficult if not impossible to make a Nb-coating of the inside surface. In the design of the cavity presented in this paper, the shape has been adapted to the Nb-coating process by providing access to the inner part of the cavity through the input and output beam pipes of a cross-section smaller than the cross-section of the central part which forms a resonator based on a piece of a double-ridged waveguide.

### Transverse Cross-section of the Cavity

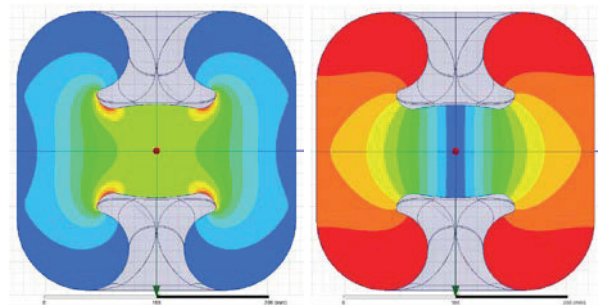


Figure 1: Transverse distributions of electric (left) and magnetic (right) fields in the middle of the cavity are presented in linear scale for deflecting voltage value of 3 MV. Maximum electric and magnetic field values on the plots (red) are 30 MV/m and 25 kA/m, respectively.

The transverse cross-section of the central part of the cavity is shown in Fig. 1 together with the electric and magnetic field distributions calculated using HFSS [3] on the left and on the right hand sides, respectively. In order to reduce the transverse dimensions of the double-ridged waveguide for given cut-off frequency close to 400 MHz,

the capacitive loading has been increased by introducing two curved plates above and below the beam aperture. The plate shape is optimized both to reduce the surface electric field and to improve the deflecting field quality by minimizing its sextupolar component  $b_3$  [4]. The shape of the waveguide outer walls has been optimized to minimize both the surface power loss and its width and height which are limited to only 252 mm in the presented design.

### 3D Shape of the Cavity

The transverse cross-section described above is swept along the cavity axis over a certain length and terminated on both sides by two 30-degree tapers, which are followed

by two rounded square beam pipes. In Fig 2, a cut through the cavity kick plane is presented together with electric and magnetic field distributions. The length of the central part forming a resonator is about 550 mm. It is optimized in order to obtain maximum shunt impedance of the deflecting mode at 400 MHz, which results in the  $R/Q$  values of  $343 \Omega$ . After the optimum length of the ridges was found, the quality of the deflecting mode has been checked and corrected by changing the curvature radius of the plates facing the beam. For total deflecting voltage of 10 MV, the sextupolar component has been minimized down to  $b_3 = -89 \text{ mT/m}$  which is much better than the beam dynamics requirements [4]. The value of the next non-zero multipolar component:  $b_5 = -1.4 \text{ kT/m}^3$ .

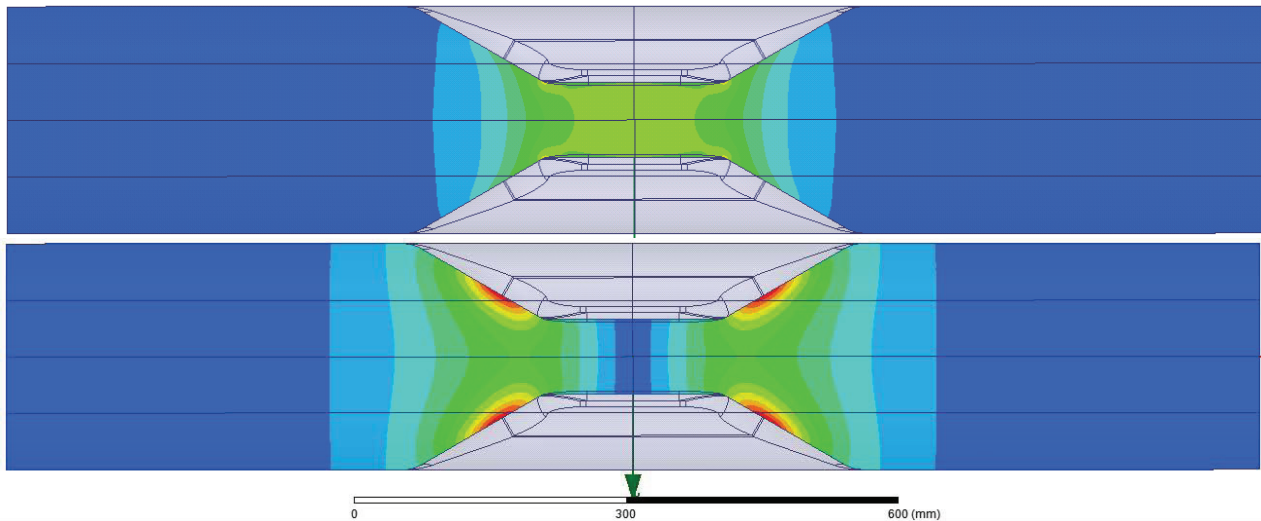


Figure 2: Electric (top) and magnetic (bottom) field distributions in the cavity kick plane are presented in the same scale as in Fig 1.

Maximum surface electric and magnetic fields are located in the region of transition from ridged-waveguide to the tapers. Their values are 45 MV/m and 68 mT, respectively, at the deflecting voltage of 3 MV. The taper angle of 30 degree has been chosen in order to facilitate the Nb-coating process. The overall length of the cavity is 1.4 m. At this length the fundamental mode field exponentially decays to a level at which a flange or any other termination does not affect significantly the cavity frequency nor the expected cavity power loss at 4.5 K.

### RF Power Loss Calculation at 4.5 K

The RF power loss on the cavity walls at 4.5 K in the superconducting state cannot be calculated directly using complex eigenmode solvers like HFSS due to very low surface resistance. It is much more accurate to calculate the Q-factor of the cavity assuming Cu conductivity at room temperature and then scale it by the ratio of surface resistances of Cu at 300 K ( $R_s^{Cu} = 5.2 \text{ m}\Omega$ ) and that of the Nb-on-Cu-coating at 4.5 K. Typically, this surface resistance shows a non-linear dependence on the surface magnetic field  $B_s$  which can be fitted by an exponential

function based on the measurements done for the LHC main RF system cavities [5]:

$$R_s^{LHC} [n\Omega] = 54.7 + 19.0 \exp(54 B_s [T]). \quad (1)$$

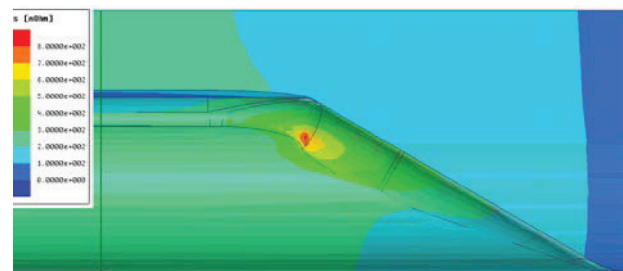


Figure 3: Surface resistance distribution of Nb-coating on the cavity walls at 3 MV obtained from Eq. (1).

The distribution of the surface magnetic field on the cavity walls is not homogeneous. This together with Eq. 1 lead to even more non-homogeneous distribution of the surface resistance of the Nb-coating which is shown in Fig. 3 for the deflecting voltage of 3 MV. According to Fig. 3,

most of the cavity walls have surface resistance of about 250 nΩ. Taking this value for the scaling of the cavity Q-factor results into the cavity Q-factor of 4.3e+8 and the total RF power loss of 60 W. On the other hand, Fig. 3 clearly shows some hot spots where the surface resistance reaches 800 nΩ as well as rather large areas on the cavity walls where it is much lower than 250 nΩ. In order to assess the impact of the non-homogeneous distribution of the surface resistance on the overall RF power loss, the power loss has been calculated in a different, more accurate way than it is described above, namely by integrating the surface power loss density calculated for Cu at 300 K and scaled locally by the ratio of the  $R_s^{Cu}/R_s^{LHC}(B_s)$  using HFSS field calculator. This results in the total RF power loss of 57 W and the Q-factor of 4.6e+8 demonstrating rather good agreement with the previous calculation.

### Beam-coupling Impedance

The smooth 30-degree tapers and the large cross-section beam pipes provides naturally efficient HOM damping and rather low beam coupling impedance. The longitudinal loss factor of 0.035 V/pC; the dipole kick factor in the kick plane of 3.5 V/pC/m and the dipolar kick factor in the other plane of 0.3 V/pC/m have been calculated for a RMS bunch length of 50 mm using CST Particle Studio [6]. The results of beam coupling impedance simulations are presented in Fig. 4 demonstrating almost HOM-free behaviour. There are only a few HOMs which requires an additional damping.

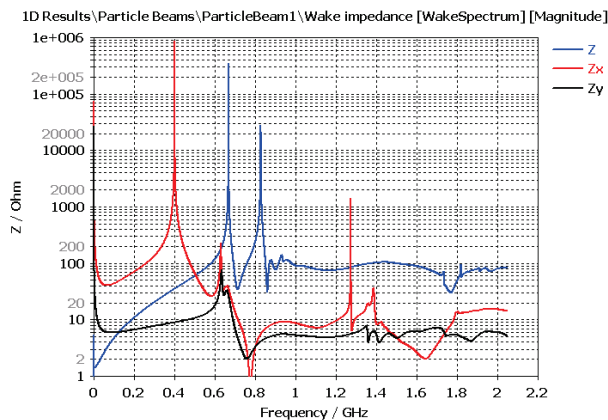


Figure 4: Beam coupling impedance: longitudinal (blue) and transverse dipolar with an offset of 10 mm both in the plane of kick (red) and in the other plane (black).

## ENGINEERING DESIGN

The fabrication and use of the cavity in a real environment require that the RF optimized surface is realized into a copper volume able to evacuate heat and sustain the loads. Indeed, such a volume must also be actually machinable, weldable and must fit in LHC constraints.

### Heat Evacuation

The cavity is designed to work at 4.5 K. At that temperature the heat exchange must be high enough to evacuate all the heat generated internally, but low enough to avoid film boiling of helium.

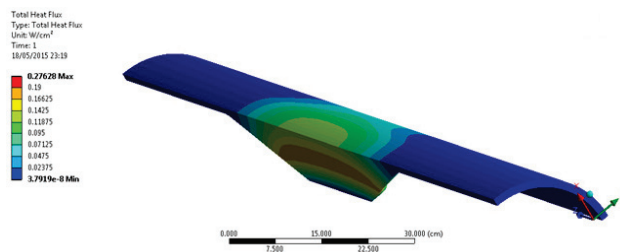


Figure 5: Computations of heat flux to helium bath.

FE calculation of the heat flux shown in Fig. 5 suggests that the peak value of the heat flux to the helium bath is below about 0.15 W/cm<sup>2</sup>, which means the thermal gradient at the helium-copper interface is about 0.2 K. Heat transfer will take place in nucleate boiling regime [7]. An additional increase of temperature of 0.4 K occurs between the surfaces in contact with helium and the cavity inner surfaces.

### Mechanical Performance and RF Sensitivity to Pressure

The capability of the cavity concept to sustain loads is assessed by means of simulation in ANSYS [3]. Indeed, this is an iterative process between mechanical and simplicity requirements and the needs of fabrication.

The loads that are applied onto the cavity during normal operation are:

- Gravity.
- 1.2 bar of pressure, from the outside. Such a value is not constant and has an oscillation whose magnitude is 0.1 bar worst-case. The first value will be called static pressure, while the second dynamic. It is worth noting, however, that the dynamic contribution is in reality a quasi-static one.

It is clear that the cavity must be able to sustain gravity and static pressure (also against buckling). On top of that, dynamic pressure affects the RF behaviour. While a static contribution can be easily corrected, continuous correction of the frequency is not straightforward. In the first tests, no tuning system is foreseen. The RF input system of the test bench at SM18 at CERN is able to follow changes in cavity eigenmode up to 400 Hz. In order to safely comply with this number against all the uncertainties, it has been decided to conceive a cavity theoretically capable of 10 times better, i.e. 40 Hz variation when 0.1 bar pressure is applied also expressed as 0.4 Hz/mbar.

There are two ways for obtaining such a performance. The first one is to design a cavity as stiff as possible by increasing the thickness of the wall. The second is to optimize the shape in such a way that the deformation due to dynamic pressure has a low effect on the 1st eigenmode.

Very thick cavity walls result in significant integration issues, not to mention the higher cost and the difficulty in joining cavity pieces during fabrication. LHC beams at the theoretical cavity location are 194 mm apart. To allow passage of the 2nd beam pipe it is required that the transverse space a distance of >145 mm from the electric centre line of the cavity is kept clear. A very compact design of the cavity in transverse direction is needed. If the cavity shape allows both vertical and horizontal kick, the constraints mentioned above must be projected on both vertical and horizontal plane. Fig. 6 shows how the cross-section is, if the external shape is made symmetrical.

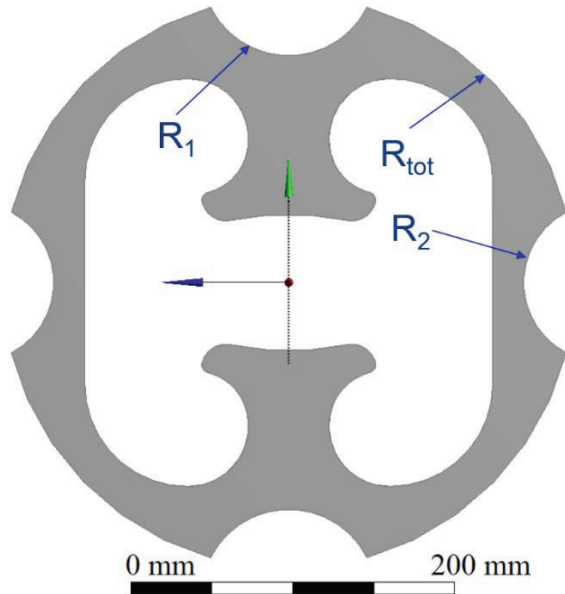


Figure 6: Transverse cross-section of the cavity. The parameters are used to optimize the shape against sensitivity to pressure fluctuations.

The external surface is cylindrical as it requires less machining and is roughly stiffer. The cylinders with radius  $R_1$  and  $R_2$  accommodate the second beam axis. The analysis of sensitivity of the cavity eigenmode to deformation shows that, Fig. 7, a change in the distance between the ridges ( $dx$ ) produces  $-2.1$  kHz/ $\mu\text{m}$  while a change in the side ( $dy$ ) results in  $1$  kHz/ $\mu\text{m}$ .

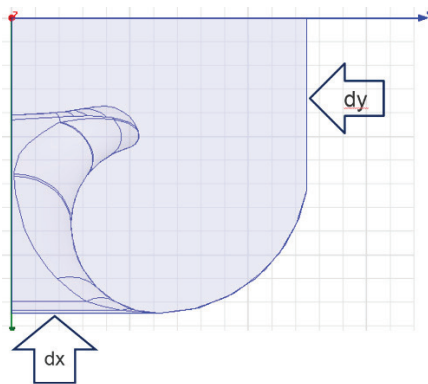


Figure 7: HFSS model for estimating eigenmode dependence on local deformations.

This means that, in principle, if  $dy = -2.1 dx$  the drift in cavity eigenmode is 0. By properly playing with the value of  $R_1$  and  $R_2$ , it is possible to find a cavity shape whose sensitivity to pressure is nominally 0. As an example a set of optimal parameters is:  $R_{\text{tot}} = 176.6$  mm (i.e. a min thickness of 25 mm),  $R_1 = 49$  mm,  $R_2 = 54.1$  mm. Indeed, a first estimation based on the  $-2.1$  factor must be fine-tuned with a set of RF numerical calculations in which the undeformed and deformed geometries are exported from ANSYS into HFSS and characterized in terms of 1<sup>st</sup> mode.

It is numerically impossible to obtain accurate results for a low pressure such 0.1 bar. The process is therefore performed for a set of values that goes from 1 to 10 bar and then scaled. The use of several values also helps minimizing the effect due to numerical errors. As general guideline, the mesh must be as similar as possible for all pressures.

This procedure is being tested and will be applied on the final shape, which is machinable and assemblable. Fig. 8 shows the rendering of a possible solution, although not fully detailed yet. The grooves are needed to allow the weld of 3 pieces. It is not possible to achieve a high machining accuracy keeping the 1.4 m cavity in one single piece.

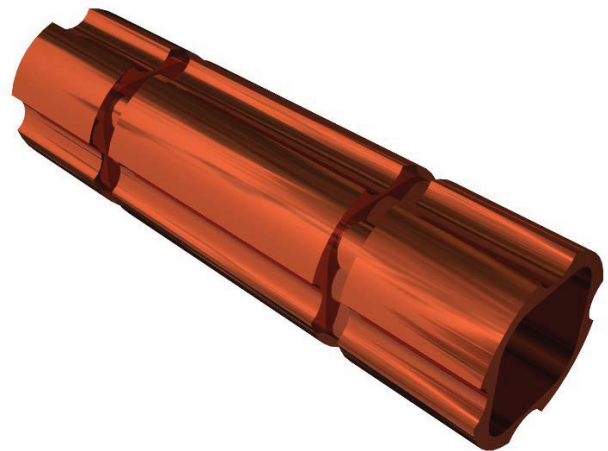


Figure 8: Cavity assembly concept.

## COATING

### Coating-friendly Cavity Design

The RF and mechanical designs of the prototype cavity have been optimized for being coated. Sharp edges and small radius of curvature shapes are avoided, potential shadowing areas are reduced, keeping the RF integrity of the cavity.

Considering the complex geometry of the kick plane, numerical simulation using MolFlow+ [8] ray tracing algorithms have been performed. Uniform emission of sputtered atoms coming from the cathode towards the surface of the cavity without binary molecular collisions has been assumed. These simulation conditions could be transposed to hypothetical case of sputtered atoms transport in low pressure magnetron sputtering

environment where the mean free path is much larger than the cathode to substrate distance.

To evaluate if the tapering and the shape of the ridged waveguide, especially in the regions of high power losses, impact on the coating uniformity (atomic flux or number of “hits” at the surface) and the film growth at the surface (atomic impinging angle at the surface), different cases have been envisaged by changing the cathode number, size and position. Fig. 9 presents an example of possible cathode configuration.



Figure 9: Possible cathode configuration with seven cathode rods of niobium.

Figure 10 shows results about angular distribution of sputtered atoms. Where the surface power density dissipated by the cavity is the highest, niobium film quality is critical and low impinging angles are required. The average angle remains low enough on the whole cavity to aim for coating quality comparable to the LHC type coating taken as reference.

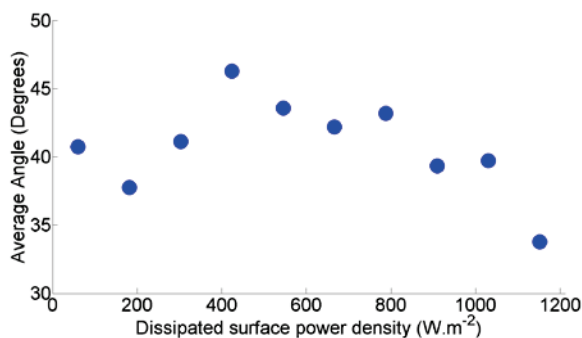


Figure 10: Averaged angular distribution of sputtered atoms impinging on the cavity wall correlated to the dissipated surface power density.

### Coating Techniques and Setup

Different coating techniques might be applied to such geometry. DC magnetron sputtering would be the first option, HiPIMS [9] is possible if adaptable to this substrate geometry. The obvious advantage of HiPIMS as compared to magnetron sputtering being the possibility to grow a uniform film all over the length/form of the cavity by combining the sputtered species ionisation and biasing of the substrate, thereby allowing conformal deposition with a normal angle of incidence everywhere [9].

The coating setup could be adapted from the one used for the HIE-ISOLDE cavities production [10] allowing a pre-coating bake-out to degas as much as possible the massive copper substrate (about 350 kg) and make coating at high substrate temperature (up to 650°C) with limited amount of hydrogen in the UHV chamber.

A simpler alternative would have been, as for LHC cavities coatings, to use the cavity itself as a vacuum chamber. However we believe that the in-situ bake-out of the substrate before coating helps in achieving higher RF performances by diminishing the amount of impurities embedded in the film during the coating process and by allowing high substrate temperature coating.

### REFERENCES

- [1] High Luminosity Large Hadron Collider (HL-LHC), website: <http://hilumilhc.web.cern.ch>
- [2] H R. Calaga et al., “Crab Cavities for the LHC Upgrade,” Proceedings of Chamonix, Chamonix, France (2012).
- [3] ANSYS HFSS, website: <http://www.ansys.com>
- [4] J. Barranco Garcia et al., “Study of Multipolar RF Kicks from the main deflecting mode in Compact Crab Cavities for LHC”, TUPPR027, Proceedings of IPAC’12, New Orleans, LA, USA (2012).
- [5] S. Aull, S. Calatroni, private communication.
- [6] CST, website: <https://www.cst.com/>
- [7] Steven W. Van Sciver, “Helium cryogenics”.
- [8] R. Kersevan, J.-L. Pons, J. Vac. Sci. Technol. A, 27 (2009), pp. 1017–1023.
- [9] S. Calatroni, Physica C 441 (2006) 95-101.
- [10] N. Jecklin et al., TUP073, Proceedings of SRF’13, Paris, France (2013).